Journal of Archaeological Science 96 (2018) 148–161

Contents lists available at ScienceDirect

Journal of Archaeological Science

journal homepage: www.elsevier.com/locate/jas

Aboriginal stone-walled intertidal fishtrap morphology, function and chronology investigated with high-resolution close-range Unmanned Aerial Vehicle photogrammetry

Anna Kreij[a,b,*], Jason Scriffignano[b,c], Daniel Rosendahl[b], Texas Nagel[a,b], Sean Ulm[a,b]

[a] ARC Centre of Excellence for Australian Biodiversity and Heritage, James Cook University, PO Box 6811, Cairns, QLD 4870, Australia
[b] College of Arts, Society and Education, James Cook University, PO Box 6811, Cairns, QLD 4870, Australia
[c] Dynamic Spatial Solutions, 106 Western Street, Rockhampton, QLD 4700, Australia

ARTICLE INFO

Keywords:
Fishtraps
High-resolution photogrammetry
UAV
GIS
Standardised recording
Quantitative analysis
Sea-level modelling
Aquaculture

ABSTRACT

Stone-walled intertidal fishtraps surround the Australian coastline and are among the largest structures built by Indigenous Australians. Globally, fishtraps are considered important elements in food production, domestication, territoriality and ceremonial landscapes, yet the level of detail in documentation is highly varied and scholarly fishtrap knowledge sparse. Comparative analysis is currently restricted by a lack of detail and reproducibility in recording, hindering analysis of morphology, function and chronology. In this study we employ high-resolution close-range Unmanned Aerial Vehicle (UAV) photogrammetry and a suite of spatial information analytical techniques to investigate the Kaiadilt Aboriginal stone-walled intertidal fishtraps of Sweers Island, southern Gulf of Carpentaria, Australia. Tidal inundation modelling is undertaken to assess (1) fishtrap working range, (2) individual and simultaneous trap function, (3) seasonal functionality and (4) chronology based on function relative to sea-level history. Thirteen fishtraps were identified in the study area, ranging from 38 m to 287 m in length. Flow accumulation indicates that shape and placement of fishtraps reflects underlying topography. Inundation modelling shows that all fishtraps operate most efficiently at present mean-sea level (PMSL), indicating construction in the last 3500 years. Quantitative recording techniques, analytical procedures and terminology developed in this study provide an opportunity to improve approaches to recording large-scale stone features and standardise documentation of stone-walled intertidal fishtrap sites.

1. Introduction

Stone-walled intertidal fishtraps are some of the largest structures documented in the Australian archaeological record. Constructed with rock and/or organic matter, fishtraps are argued to be primarily designed to trap or control the movements of marine resources across tidal cycles in coastal or riverine contexts (Campbell, 1982; Dortch et al., 2006; Jeffery, 2013; Rowland and Ulm, 2011). For the purposes of this study, stone-walled intertidal fishtraps are defined as structures capable of controlling the movements of marine animals.

Fishtraps, as structures testifying to local subsistence, labour organisation, occupation, and social strategies, have been cited as features of early domestication (Codding and Bird, 2015; Smith, 2014; Zeder, 2015), anthropogenic niche construction (Lepofsky and Caldwell, 2013; Lourandos, 1980; Smith, 2014; Zeder, 2015), and Australian mid-to-late Holocene economic and social intensification (Lourandos, 1980, 1983; McNiven et al., 2012, 2015). Despite interest across the fields of archaeology, evolutionary biology, and human behavioural ecology, physical and conceptual challenges of characterising fishtraps have led to a variety of approaches to site recording. As a result, researchers often adopt vague fishtrap definitions and terminologies (Bannerman and Jones, 1999; Jeffery, 2013; Ross, 2009; Rowland and Ulm, 2011), and fundamental questions concerning fishtrap construction and function are yet to be addressed (Caldwell et al., 2012; Elder et al., 2014; Moss et al., 1998).

Due to the location of fishtrap structures in intertidal and riverine settings, access is often restricted and dependent on tidal movement, and in certain parts of the world the presence of marine predators can be hazardous to field researchers. Recording time and visibility is also controlled by tides, and can further be restricted by wind, causing swell and sediment to obscure structures. Such environmental factors, along with the impacts of recreational marine vessels, cause intertidal stone

* Corresponding author. ARC Centre of Excellence for Australian Biodiversity and Heritage, James Cook University, PO Box 6811, Cairns, QLD 4870, Australia.
E-mail addresses: anna.kreij@my.jcu.edu.au (A. Kreij), jason@dynamicss.com.au (J. Scriffignano), danrosendahl@gmail.com (D. Rosendahl), texas.nagel@my.jcu.edu.au (T. Nagel), sean.ulm@jcu.edu.au (S. Ulm).

https://doi.org/10.1016/j.jas.2018.05.012
Received 8 May 2018; Received in revised form 29 May 2018; Accepted 29 May 2018

features to erode partially or completely, which underlines the urgency in recording remaining fishtrap structures (Elder et al., 2014; Memmott et al., 2008; Roberts et al., 2016; Rowland and Ulm, 2011; Rowland et al., 2014). Despite the urgency of documentation, and a global interest in fishtrap construction (e.g. Greene et al., 2015; Jeffery, 2013), most recordings consist of basic sketch maps of limited detail, with few quantitative data or photographic records (for exceptions see Coutts et al., 1978; Greene et al., 2015; Koivisto et al., 2018; Langouët and Daire, 2009; McNiven et al., 2012; O'Sullivan, 2004). Varied approaches to site recording has led to a proliferation of terms describing fishtrap attributes, which pose challenges for site management, comparison of sites, and the ability of fishtraps to be considered meaningfully in broader debates. This study focuses on intertidal stone-walled fishtraps and proposes a standardised high-resolution recording scheme for large-scale intertidal stone features, to improve knowledge of fishtrap construction, function, and age.

2. Background

In 2011, Rowland and Ulm published a comprehensive review of coastal and inland fishtraps and weirs in the state of Queensland, Australia. The review found that stone-walled fishtraps are generally situated on coastal points or estuaries sheltered from strong winds, and while limited, evidence indicated that organic traps and weirs were generally located inland. Multiple pens (or holding areas) are observed in the Torres Strait and Gulf of Carpentaria, while isolated single pen structures are found further south. Most coastal fishtrap structures across the state displayed an arc shape, and it was recognised that traps were constructed and utilised by both Indigenous and non-indigenous Australians (Rowland and Ulm, 2011). The authors concluded that the level of detail available in Queensland fishtrap recording was largely substandard and proposed standardised recording schemes with increased detail in documentation (Rowland and Ulm, 2011).

Rowland and Ulm's (2011) findings apply to Australia more broadly, where site comparison is challenged by uncertainty in identification, a variety of recording techniques, and a wide range of associated terminology. Australian intertidal stone-walled fishtrap documentation is dominated by sketch maps to varied detail of fishtrap location, shape, and dimensions. More sophisticated documentation techniques and global navigation satellite systems (GNSS) have only been adopted in recent ground and aerial documentation strategies. While the recommendation by Rowland et al. (2014) to utilise Light Detection and Ranging (LiDAR) to capture large-scale coastal sites in detail has not yet been adopted in the Australian fishtrap context, various aerial recording techniques have been trialled. Low-level aerial photography was utilised in fishtrap site identification and analysis by Campbell (1982) at Hinchinbrook Island, Queensland, Dortch (1997) at Wilson inlet, Western Australia, and by Connah and Jones (1983) and Memmott et al. (2008) in the Gulf of Carpentaria. Photogrammetry, today a well-established technique in three-dimensional (3D) modelling (Sapirstein, 2016), has been sparsely applied in Australian fishtrap literature. The technique, allowing the generation of geometrically accurate photo-mosaics from which precise measurements can be retrieved, was used by Smith (1987) in a close range (< c.300 m) ground photo mosaic of a Bardi fishtrap, Dampier Peninsula, Western Australia, which provided a detailed map of the trap to scale. The anthropogenic inland stone-walled structures of Gunditjmara country, Lake Condah, southwest Victoria, have received the most detailed documentation to date. Van Waarden and Wilson (1994) used aerial photogrammetry (> c.300 m) to map the region, creating 1 m contoured topographic maps (1:5000), followed by Richards' (2013) detailed surface mapping using Real-Time Kinematic (RTK) Differential GNSS (DGNSS), and Builth's (2014) use of the same technology to create a 2 m × 2 m digital elevation model (DEM) for sites within the lava flow.

The various recording techniques applied in fishtrap studies have led to a wide range of terminology across the literature. While some studies describe stone-walled structures by physical composition (e.g. *alignment* by Dortch et al. (2006), *continuous walls* by Stockton (1975) or observed or perceived function e.g. *barrier* by Roberts et al. (2016)), the majority of studies focus on the morphology of structures. Aligning with Rowland and Ulm's (2011) findings, the *arc* (also described as *U-shape* or *semi-circular*), and *circular* terms are the most common shape characteristics applied across Australian fishtrap publications. Such morphological descriptors are problematic owing to their arbitrary and subjective nature, and risk neglecting or recording multiple traps as single features, and vice versa (e.g. one w-shaped trap or two v-shaped, or semicircular traps). Dimensions generally consist of a measure of the tallest and widest points of the trap, and an east-west and north-south measure of the enclosed area, but complete metrics are rarely presented for individual sites. Focusing on shape and size, fishtrap assessments generally neglect 3D aspects of structures, with the exception of Campbell (1982) who estimated holding capacity of the Scraggy Point fishtrap complex on Hinchinbrook Island. Although Campbell's (1982) early volume calculations assume homogenous wall height and a uniform substrate, it provides the only quantitative estimate of a fishtrap complex's holding capacity in the Australian literature.

The most significant challenges facing Australian fishtraps concern documentation, monitoring and management. The risk of structural degradation of fishtraps is an urgent practical implication of increasing coastal developmental pressures and climatic impacts (Memmott et al., 2008; Roberts et al., 2016; Rowland and Ulm, 2011). These threats cannot be appropriately managed without knowledge of current status of the intertidal stone-walled structures. To improve understandings of fishtraps, this study applies high-resolution Unmanned Aerial Vehicle (UAV) photogrammetry to document the stone-walled intertidal fishtraps of Sweers Island, southern Gulf of Carpentaria, Australia.

3. Methods

3.1. Case study area

The stone-walled intertidal fishtraps of Sweers Island are situated on the traditional lands of Kaiadilt people in the South Wellesley Islands, comprising an archipelago of 10 islands with Sweers Island the easternmost (c.13 km^2) (Fig. 1). A local sea-level curve for the southern Gulf of Carpentaria demonstrates that rising post-glacial sea-levels separated the islands from the mainland c.8000 cal BP (Sloss et al., 2018). At 7700 cal BP sea-levels reached present mean sea level (PMSL), continuing to increase to +1.5 m-2 m above PMSL, with relatively stable sea-levels remaining until 4000 cal BP. Sea-levels rapidly regressed to 0.5 m ± PMSL between 4000 and 3500 cal BP (Sloss et al., 2018). The earliest documented occupation of the South Wellesley Islands occurs at 3483 cal BP on Bentinck Island and 3421 cal BP on Sweers Island, with a continuous occupation signal from around 2000 cal BP and strong evidence for permanent occupation in the last 1000 years (Memmott et al., 2016; Peck, 2016; Ulm et al., 2010). Archaeological and ethnographic evidence indicate that Bentinck Island was the focus of residence, with smaller surrounding islands, such as Sweers, visited for resource extraction and temporary occupation (Evans, 1995; Memmott et al., 2016; Tindale, 1962a; Ulm et al., 2010). The Kaiadilt population, believed to have reached a maximum of 123 individuals (Tindale, 1962b), were forcibly removed to a European mission on Mornington Island in 1948. Kaiadilt were the last coastal Aboriginal group to be institutionalised in Australia (Memmott, 1982).

The South Wellesley Islands generally experience a diurnal tidal range (one high and low tide each day) of approximately 3 m in amplitude, with an exception every fortnight where 'double' tides occur for 1–3 days, resulting in little water movement (Forbes and Church, 1983). Tidal fluctuations are most prominent during the wet season due to the strong northeast winds (Memmott, 1982). However, the southern part of the Gulf can experience varied tidal patterns when the combined effects of the shallow basin, strong winds, atmospheric pressure, and

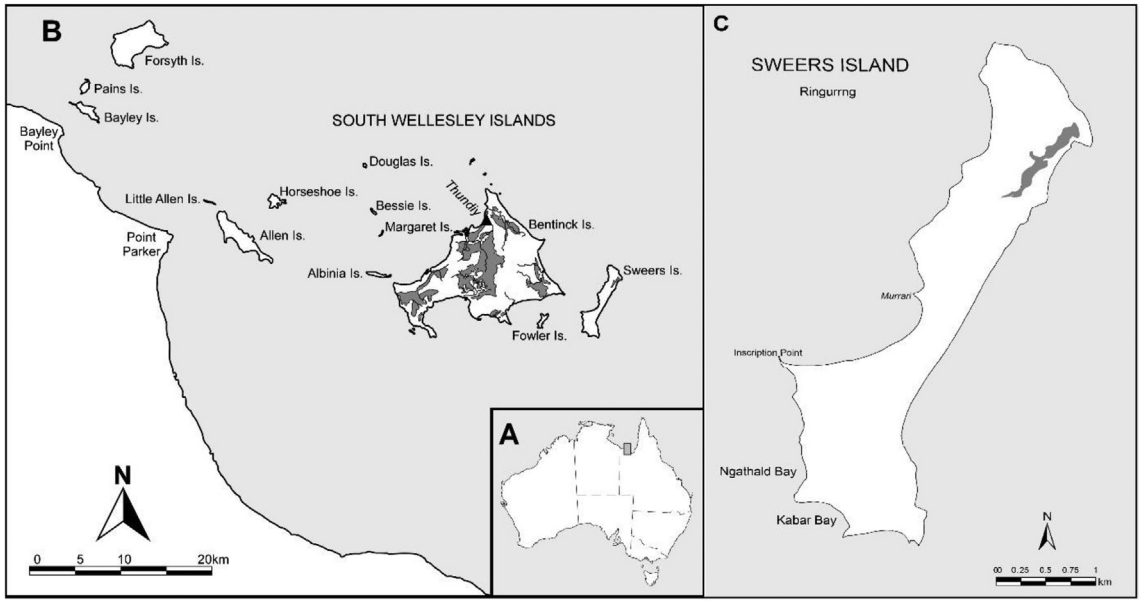

Fig. 1. (A-B) South Wellesley Islands in the Gulf of Carpentaria, northern Australia. (C) Sweers Islands, the most eastward island in the archipelago. Kayardild place names are adopted from Memmott's (1982) site map (which is reproduced in Robins, 1983), with orthography after Peck (2016).

wet season run off coincide, and can halt and/or reverse typical clockwise currents, creating counter-clockwise currents and unpredictable tidal patterns (Forbes and Church, 1983). The extensive fishtrap structures (or *ngurruwarra* in Kayardild language) of the South Wellesley Islands have been described by several authors (Evans, 1995; Memmott et al., 2008, 2016; Robins, 1983; Saenger and Hopkins, 1975; Tindale, 1962a, 1962b). The first records of the Sweers Island fishtraps appear in Saenger and Hopkins (1975), who identified one fishtrap in Kabar Bay, one in Ngathald Bay and a third on the central eastern side of the island, later identified as the named *Murarri* trap (Robins, 1983). After an archaeological survey by Memmott and Robins in 1982, the number of reported fishtraps increased, later confirmed by low-level aerial photography as eight structures present on the island (Memmott et al., 2008), however the sites were not recorded in detail (Robins, 1983).

3.2. Photogrammetric UAV survey

In September and October 2015, fishtrap structures in Ngathald and Kabar Bays on the southwest Sweers coastline (Fig. 1) were subject to close-range photogrammetry utilising a Dynamic Spatial Solutions custom-built carbon frame octocopter. The UAV, equipped with 16" propellers, T-Motor U5 motors, a MikroKopter flight controller with GNSS, carried a 3 axes brushless gimble supporting a 24 megapixel DSLR Sony A6000 with a 20 mm prime lens (26.5 mm × 15.6 mm sensor). The vehicle was powered by 22Ah 6S or 16Ah 7S lithium polymer batteries, resulting in a total take-off weight of 8 kg. Five eight hectare (Ha) flight areas generated in ESRI ArcMap (10.2.1), utilising ESRI ArcGIS Online Gallery and Google Earth (v7.1.7) satellite imagery to determine survey boundaries, were exported to the mounted flight controller, providing a pre-programmed flight path, flown at 55 m elevation at a speed of 6 m/sec (Table 1) by Civil Aviation Safety Authority (CASA) certified pilots Michael Boland (Unmanned Aerial Vehicle Services) and Jason Scriffignano (Dynamic Spatial Solutions). Prior to recording, a permanent survey marker was established by placing a GNSS on an elevated beach ridge south of Kabar Bay (within 4 km of the survey area), to act as a base station, providing RTK geospatial corrections to a GNSS rover. To enable georeferencing of the photogrammetric model, ground controls points (GCPs), represented by numbered black and white linoleum tiles, were systematically placed at

Table 1
Details of individual Sweers Island (SW) flight areas (FA).

Flight Area	Tracks	Track Length (m)	Elevation (m AHD)	Flight Time (min)	Photographs	GCPs
SW-FA 1	10	470	55	20:30	533	18
SW-FA 2	10	370	55	16:48	422	18
SW-FA 3	9	395	55	24:01	400	18
SW-FA 4	9	412	55	16:05	414	18
SW-FA 5	10	289	55	13:56	330	12

50 m spacing in the intertidal zone and mapped with the RTK GNSS rover to retrieve high accuracy location and elevation measures (Fig. 2). Flights were conducted at 55 m elevation above the Australian Height Datum (AHD) at the lowest possible tide, daylight and weather permitted, within the timeframe of the field season, to capture the maximum extent of the stone-walled structures. Recording commenced at an outgoing tide, with tides ranging from a predicted low 1.17 m–2.62 m high above Lowest Astronomical Tide (LAT) (Table 2).

While LiDAR has been suggested for data collection in coastal environments (Rowland et al., 2014), the dynamic conditions of the intertidal zone, with both terrestrial and submerged structures, are not suited as the infra-red pulse will be absorbed by water in inundated areas. Challenges of greater recording duration and resolution in bathymetric LiDAR, designed to record features at great depths, also proved unsuitable for high-resolution mapping of shallow submerged features (Doneus et al., 2013). Baltsavias (1999) additionally suggests that higher geometric resolution is achieved with aerial metric imagery captured from the same elevation as infra-red laser LiDAR.

3.3. Data processing

UAV data were prepared for processing in Folder2List, Microsoft Excel and ArcMap by aligning GNSS camera triggers with time-stamped photographs and re-projecting image coordinates. During recording, the flight controller sent triggers to the camera to capture images, while the internal GNSS simultaneously recorded geographic position, representative of where the camera was situated when the photograph was taken. The GNSS coordinates were recorded as the trigger was sent, causing a small time-lag between the recorded location and where the

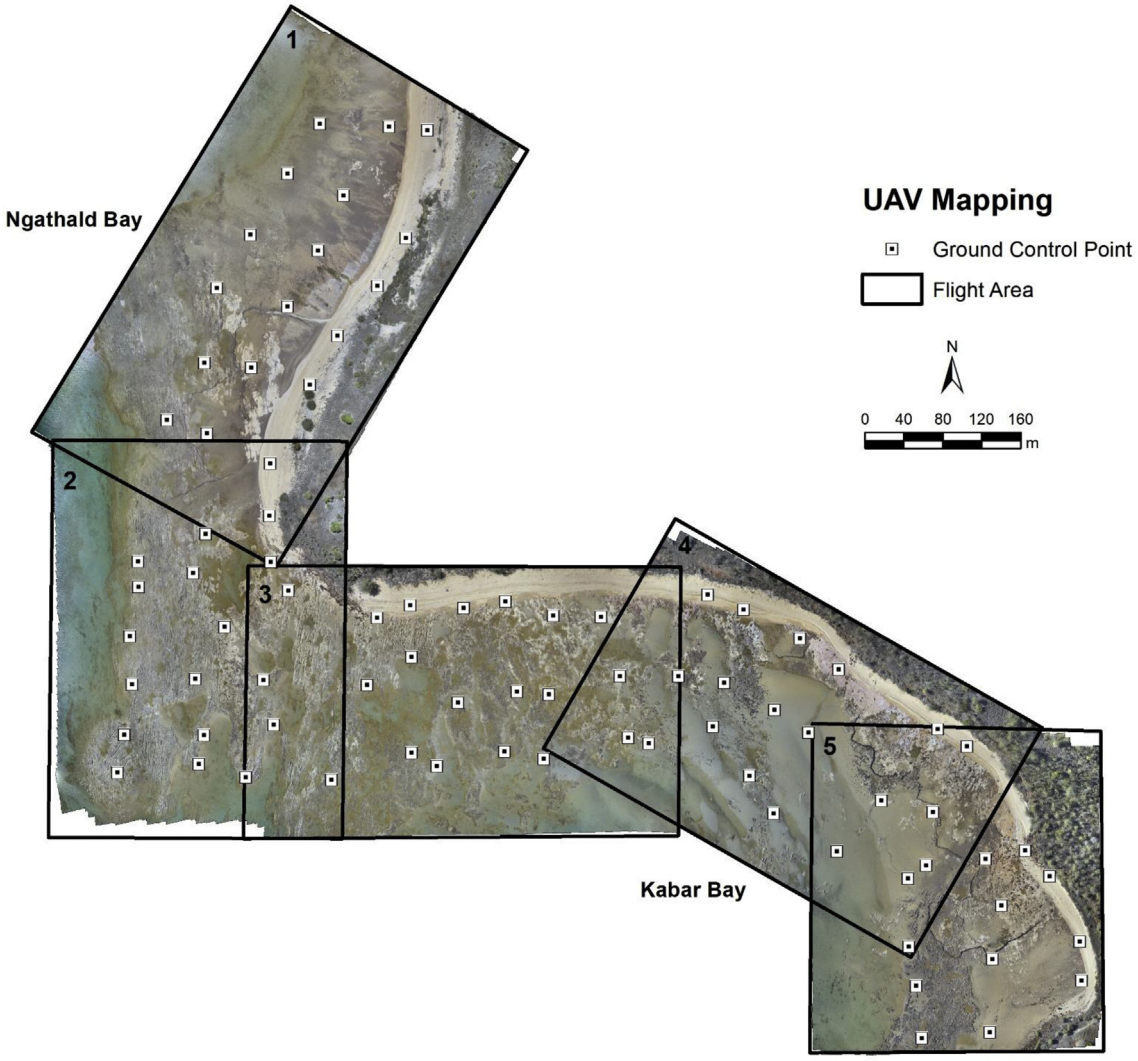

Fig. 2. Location of Sweers Island flight areas 1–5, illustrating ground control points (GCPs) (in black and white), overlaid on orthographic image generated from captured UAV data.

Table 2
Tidal range during UAV mapping. Tides as predicted for Inscription Point (Sweers Island) 2015 (DTMR, 2013).

Flight Area	Date	Recording Commenced	Time of Low Tide	Low Tide above LAT (m)	Time of High Tide	High Tide above LAT (m)
SW-FA 1	20.09.15	13:28	15:12	1.17	0:44	2.62
SW-FA 2	20.09.15	14:08	15:12	1.17	0:44	2.62
SW-FA 3	20.09.15	14:55	15:12	1.17	0:44	2.62
SW-FA 4	06.10.15	16:23	15:42	0.80	1:47	3.30
SW-FA 5	20.09.15	16:58	15:12	1.17	0:44	2.62

photograph was captured; potentially causing up to 2–3 m offset when travelling at a speed of 6 m/s, and a greater number of logged triggers than photographs. While the use of GCPs rectifies such inaccuracies during post-processing, camera triggers and photographs first require alignment to enable processing. To convert the flight controller's captured coordinates to a spatial reference suited for local-scale analysis, the aligned flight log was imported into ArcMap and re-projected into a local coordinate system, in this case Geocentric Datum of Australia 1994, Map Grid of Australia Zone 54. The projected photograph trigger coordinates were then exported as a text file and imported to Agisoft PhotoScan Professional (1.2.1) to create a 3D model of the mapped area.

To generate a point cloud, the re-projected coordinates and images from individual flights were imported into Agisoft PhotoScan Professional, software previously applied in archaeological 3D reconstructions (e.g. De Reu et al., 2013; Olson et al., 2013). A sparse point cloud was generated by aligning camera positions and applying a low-resolution mesh to create a continuous surface from which GCPs could be identified (Fig. 3). Image alignment, comprising 330–533 images per flight area, was made with high accuracy setting, generic pair selection, a key point limit of 40,000 and tie point of 1000. To georeference the model, GCPs were visually identified in individual photographs and assigned the RTK GNSS coordinates, providing a precise and accurate location and elevation value on the digital surface. The procedure was finalised by *optimising* the alignment, where camera calibrations were generated using the GCP locations, producing a 3D root mean square error (RMSE). The 3D RMSE refers to the overall error of the photogrammetric model and the actual location of individual GCPs.

To produce an orthographic image, and a DEM for further analysis of the fishtraps sites, the geo-referenced and error evaluated sparse point cloud was processed into a dense point cloud. Agisoft PhotoScan Professional generates dense point clouds through advanced image matching algorithms (see Verhoeven, 2011), computing coordinates of

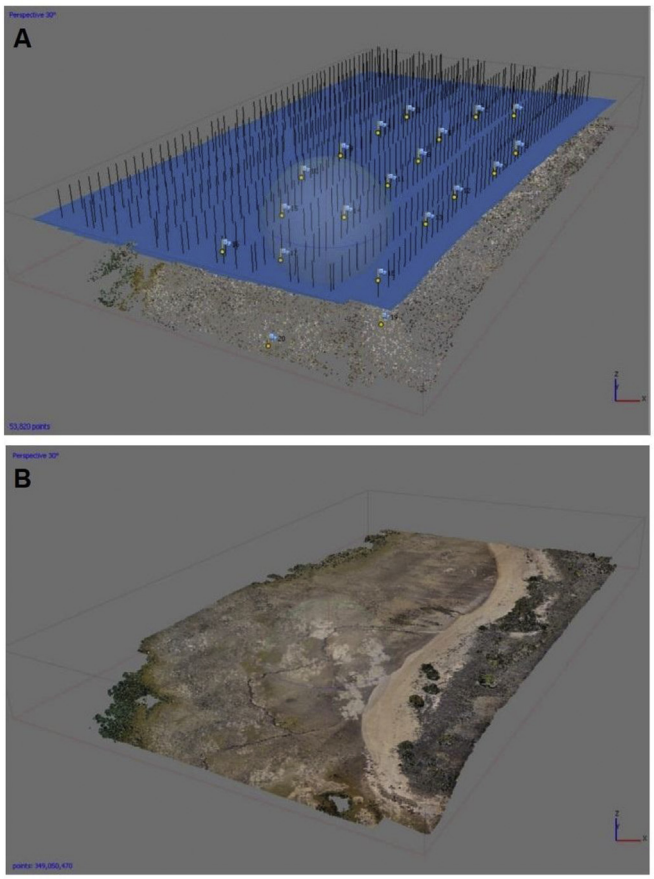

Fig. 3. (A) Sparse point cloud of flight area SW-FA1 showing camera positions (in blue) and GCP locations (n = 18), and (B) dense point cloud of flight area SW-FA1 generated in Agisoft PhotoScan Professional (1.2.1). (For interpretation of the references to colour in this figure legend, the reader is referred to the Web version of this article.)

thousands of points, resulting in a detailed 3D model of the recorded feature or site. The Sweers Island dense point clouds were individually generated with a high-quality setting and moderate depth filtering (Fig. 3), followed by merging into a single *chunk* and batch processed into a dense point cloud mosaic of the entire study area. A high precision mesh was generated to create a continuous surface, orthometrically correct the image, and generate a DEM; creating a final output of 2 cm × 2 cm pixel resolution. The orthographic image (.jpg) and DEM (.tiff), representing elevations in metres AHD, were exported for analysis of stone-walled fishtrap features.

3.4. Analytical procedure

The relationship between fishtrap placement and tidal movement was assessed in ArcMap. By importing the UAV-generated DEM to ArcMap, a raster representing slope percentage was generated (*Spatial Analyst* toolbox) to aid in identification of linear features by distinguishing low and steep gradients in the topography. Drawing on McCoy et al.'s (2011) geographical information system (GIS) methodology, four categories were established for fishtrap identification. By reclassifying slope into categories, excessive gradient was reduced, and a stronger visual representation of features was achieved. The output additionally assists in identifying the highest point of structures, as top stones are displayed as flat surfaces in contrast to the vertical walls (Fig. 4). In this study, fishtraps are defined by their ability to control movements of marine animals, and therefore ability to isolate a body of water. A contour layer was generated to identify boundaries of individual traps, based on the probability of pooling water within the structures. To establish appropriate precision in contour intervals a trial and error approach was adopted, which demonstrated the significance of fine intervals across the low gradient surface, resulting in a generation of 0.10 m contour intervals. To further assess the likelihood of pooling water, an output of flow accumulation was generated, indicating direction of water flow and likely areas of pooling.

Once the extent of fishtraps was established, individual structures were manually digitized based on the reclassified slope and contour outputs, with cross-reference to the orthographic image. Natural features incorporated in the trapping system and constructed walls were not separated in this analysis, as the purpose of this study was to assess tidal and trap correlation, rather than individual trap components. Drawing a polyline through the centre of a trap, length and elevation metrics were extracted through the *3D Analyst* toolbox. As individual traps vary in height across their construction, mean elevation of the polyline was used to establish the top elevation of fishtrap walls. To calculate the height of fishtraps, the same procedure was executed by digitising a polyline at the base of the wall facing the shoreline (Fig. 5). Minimum elevation was extracted as topography is not homogenous and water is likely to pool at lowest elevations. By subtracting minimum elevation of substrate from mean elevation of the top wall, a mean fishtrap height was calculated (Fig. 6).

To assess the current and past ability of fishtraps to enclose water, numerous tidal scenarios were simulated to determine fishtrap working ranges. Working range is taken to be the time a trap is in effective use, represented by the elevation range where fish and other mobile marine animals can theoretically be contained within individual structures (i.e. working range is the elevation between no water and walls over-topped by water). The range is determined by wall height and topography, based on the mean elevation of top wall and minimum elevation of substrate. The possibility of marine animals being collected below working range, when traps are dry, is acknowledged. However, for the purpose of comparison, tidal range exceeding or not reaching the established working range is not considered to be in effect.

To align sea-levels and the photogrammetric model in a compatible format, tidal heights required recalibration to local terrestrial heights. Tidal range predictions, in the Australian context, are referenced to a height above LAT, the predicted lowest tide of the year (Department of Transport and Main Roads (DTMR) 2017), while terrestrial heights are described as a height above AHD, an Australian datum providing vertical control in surface mapping (Geoscience Australia, 2018). Zero AHD is referenced, but not necessarily equal, to PMSL across the nation. With local PMSL variations, major ports have established height datums to enable calibration of local sea-level fluctuation. For most Australian ports, calibrated Australian National Tide Tables (ANTTs, with electronic versions referred to as *AHP11*) can be obtained by the Bureau of Meteorology (BOM) and relevant State Governments agencies. However, presumably owing to the relatively small size and remote location of Sweers Island, the case study area is not considered a major, or standard, port and does not host a local datum. Tidal predictions for Sweers Island's port Inscription Point are therefore extrapolated from mainland standard port Karumba (135 km southeast of Sweers Island) which experiences a similar tidal regime (DTMR, 2017), demonstrated by a predicted 0.04m difference in predicted mean sea-level (MSL) for the two ports from 2015. The Karumba port datum has proved reliable with an observed MSL within 0.26 m of predicted levels in 2015 (estimated mean sea-level predicted to 2.11 m, and observed levels reaching 2.37 m) (BOM, 2018). While it is not possible to calibrate a precise tidal AHD offset without long-term documentation of local coastal processes, the Karumba port data are considered adequate for inundation modelling of Sweers Island.

Prior to modelling inundation events, ANTT tidal predictions were re-calculated to AHD heights to correlate with the UAV-captured dataset. First, the predicted PMSL of 2.06 m above LAT for Inscription Point was subtracted from the Karumba port datum, where 0 m AHD is represented by 2.184 m above LAT giving a value of 0.124. This value

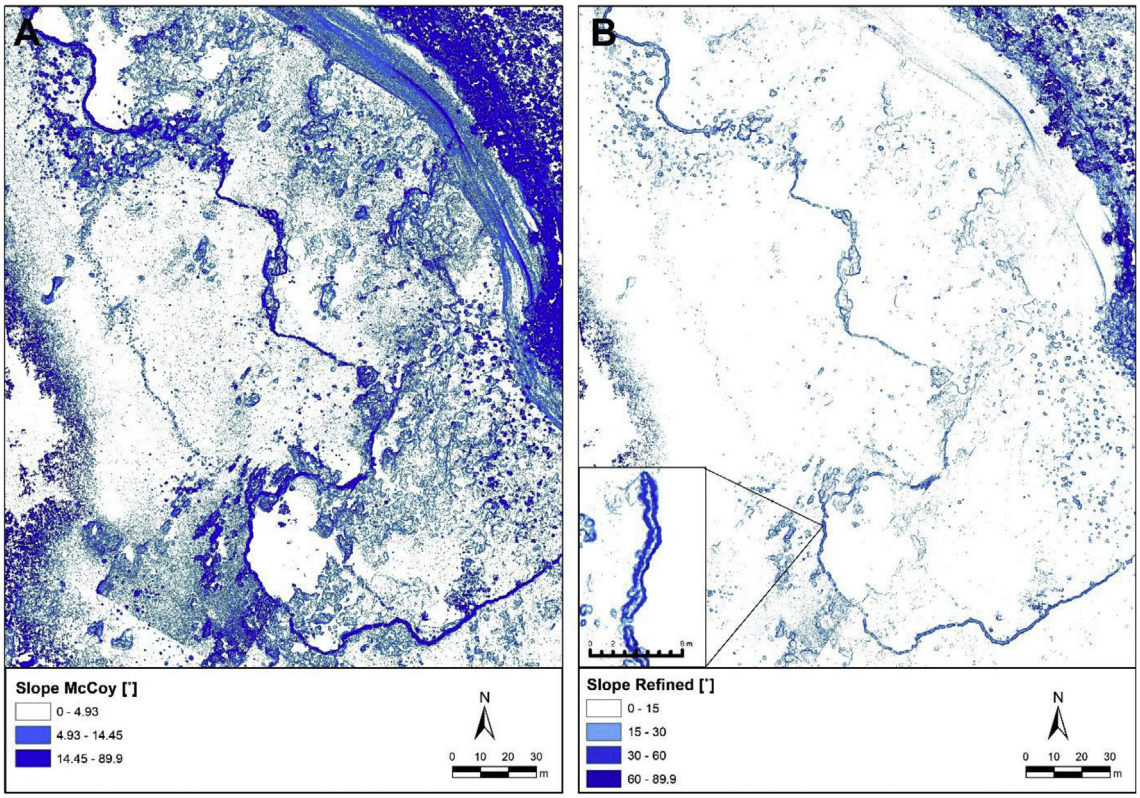

Fig. 4. DEM-generated slope outputs, reclassified after McCoy et al.'s (2011) 'slope contrast mapping' model, with (A) three categories of slope, and (B) the refined classification with four categories of slope, with inset close-up illustrating the flat appearance of the top of the wall.

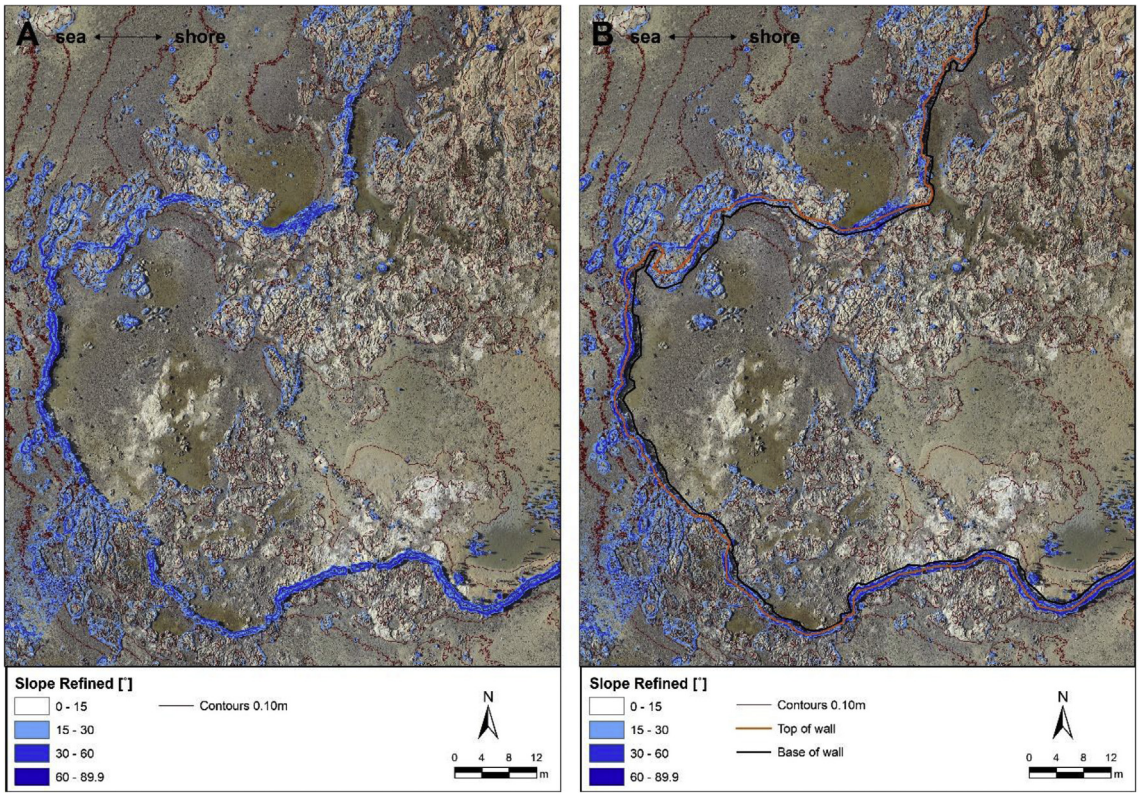

Fig. 5. (A) Slope, contours and the orthographic output assisted in individual fishtrap identification, followed by (B) digitisation of structures to retrieve wall height and elevation of underlying topography.

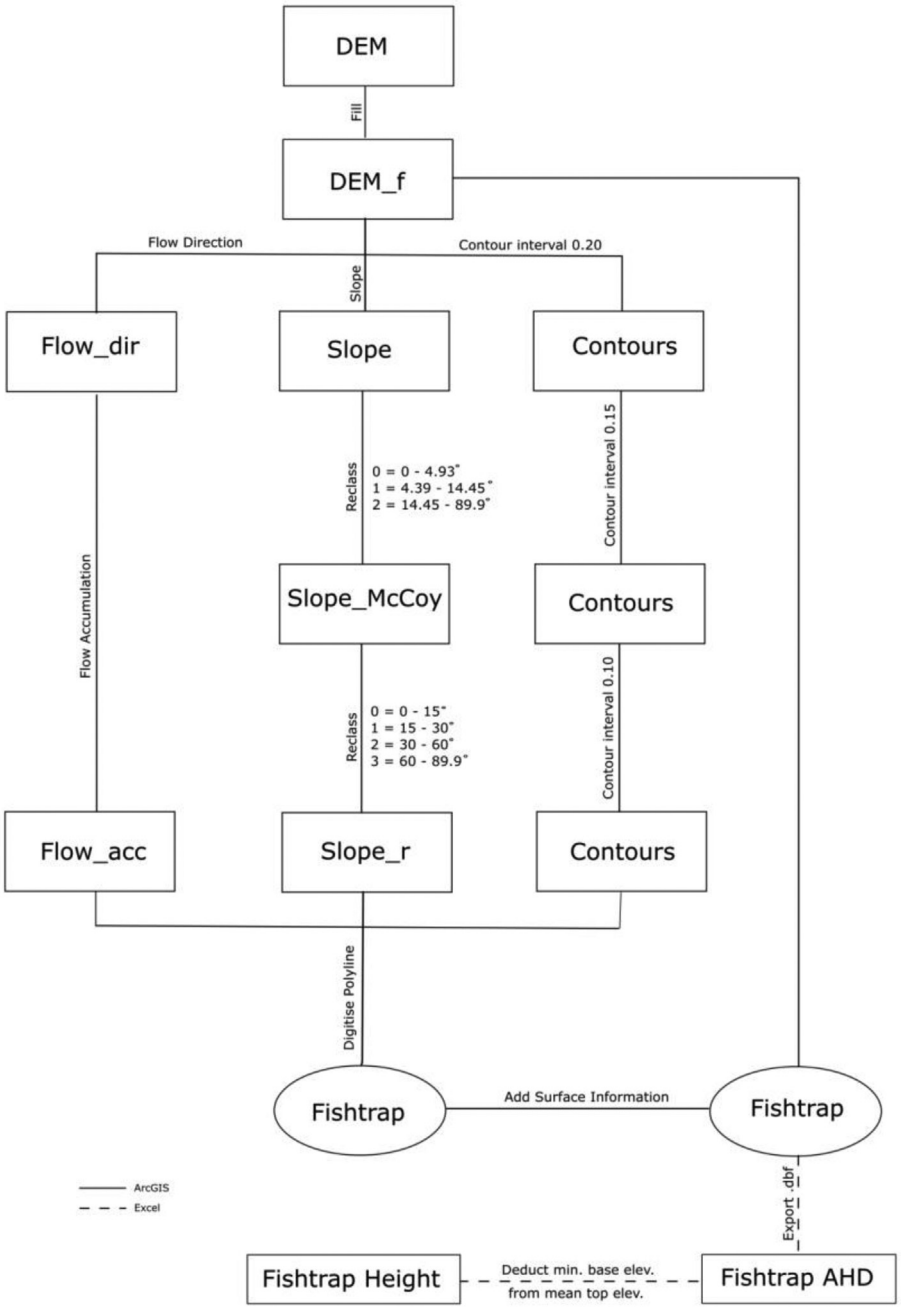

Fig. 6. GIS analytical procedure for fishtrap identification and metrics.

was deducted from 0 m AHD to give a tidal height of −0.124 m AHD. The Raster Algebra tool (*Spatial Analyst* toolbox), or raster reclassification with the same principle, have previously been utilised to visualise scenarios of sea-level rise by displaying DEM values below or above a set threshold (e.g. Kuhn et al., 2011; Lichter and Felsenstein, 2012), and was adopted for this study. To model a PMSL of −0.124 m AHD for Sweers Island, the raster tool was set to display all pixels containing values equal to or below −0.124 m. The output is a raster file containing areas that do not satisfy the criteria (0) and areas that do (1). To display the generated tide with the orthographic image, the output was reclassified to disregard values of 0 and display 1, followed by a conversion to a vector file, to reduce file size and aid drawing in ArcMap.

Modelling of tidal inundation was initially undertaken using predicted tides of the day of UAV recording, to evaluate the procedure against known conditions, followed by enhanced PMSL scenarios, and mean annual magnitude of wet and dry season regimes. Mean seasonal high tide was based on the mean of predicted higher high water (MHHW) and mean lower high water (MLHW), and low tide drawn from the mean of mean higher low water (MHLW) and mean lower low water (MLLW) of 2015 (DTMR, 2013). Following this procedure, several characteristics of function were assessed: (1) fishtrap working range, (2) individual and simultaneous trap function, (3) seasonal functionality and (4) relative timeframes of fishtrap function in relation to previous sea-levels.

4. Results

4.1. 3D root mean square error (RMSE)

The accuracy of the created imagery and DEM is defined by the magnitude of 3D RMSE. The geometric error is based on the accuracy of

the 84 RTK GNSS captured on-ground locations, post-processing positioning of GCPs in individual photographs, and photograph image quality. The resulting error estimate reflects the model's virtual position as opposed to physical location. This was also correlated by the use of interactively allocating GCPs as control or reference points during the model process, where reference GCPs displayed a comparable error in location to the 3D RMSE. Across the merged flight areas, the total 3D RMSE was less than 2.5 cm, representing a horizontal error of 0.9 cm along the x-axis, 1.21 cm across the y-axis, and 1.93 cm of vertical inaccuracy. The error was computed at a 68.27% confidence level (one standard deviation), which reflects geographical uncertainty of individual GCP. With a total 3D error below 2.5 cm, the accuracy of the model is equivalent to spatial precision provided by current RTK GNSS systems, where horizontal accuracy is estimated to 1 cm + 2 ppm (part per million) and vertical differentiation up to 2 cm + 2 ppm, when survey is situated within 10–40 km of associated base station (United States Geological Survey, 2017). The 3D RMSE demonstrates the Sweers Island fishtrap model to be close to identical to original RTK GNSS accuracy, despite its post-processing procedures. With a GNSS base station-rover distance within 4 km and a 2 cm × 2 cm pixel resolution, the maximum potential model error is equivalent to a single pixel. The 3D RMSE is therefore considered minor, and not predicted to impact spatial analysis results.

4.2. Fishtrap working range

Thirteen fishtraps were identified in the study area. The stone-walled structures are situated in the nearshore zone between 20 m and 120 m from the current high water mark, ranging from 38 m to 287 m in length, 0.15–0.97 m in height, and an average width of 0.50 m (Table 3, Fig. S1). The various working ranges of individual fishtraps, determined by topographic elevation and mean wall height, demonstrate the traps to enclose water effectively at various tides; therefore, individual traps are considered to be separate fishtrap sites. While the reasoning behind fishtrap construction cannot be confirmed, the flow accumulation strongly indicates shape and placement to reflect the underlying topography (Fig. 7). The lateritic substrate underlying most traps in the study area further provides a fixed foundation from which reliable elevation measures were calculated. The fishtraps of Ngathald and Kabar Bay are constructed between elevations of 0.35 m and −0.41 m AHD, with traps anchored to or near the modern shoreline. The majority of structures are constructed near AHD, where the physical expression of the arbitrary surface is PMSL. PMSL at Sweers Island is approximately −0.124 m AHD. By comparing PMSL and tidal scenarios to trap location, visual and numerical representations of fishtrap function can be calculated.

Table 3
Individual fishtrap properties, with *N* traps representing structures in Ngathald Bay and *K* traps in Kabar Bay.

Trap ID	Length (m)	Mean Height (m)	Mean Width (m)	Elevation Range (m AHD)	
				Min. base	Mean top
N1	38.13	0.28	0.46	−0.263	0.017
N2	61.04	0.15	0.44	−0.207	−0.060
N3	56.18	0.23	0.52	−0.411	−0.178
N4	158.52	0.30	0.48	0.350	0.651
N5	220.77	0.37	0.47	0.036	0.404
N6	196.61	0.36	0.64	−0.094	0.269
N7	117.40	0.97	0.76	−0.976	−0.006
K1	91.86	0.25	0.62	−0.172	0.080
K2	53.28	0.37	0.83	−0.147	0.219
K3	72.02	0.42	0.73	−0.081	0.336
K4	44.85	0.30	0.55	−0.407	−0.111
K5	81.10	0.30	0.54	−0.300	−0.004
K6	287.28	0.45	0.56	−0.279	0.172

4.3. Functionality

Modelling of present sea-levels demonstrate fishtrap sites to be located within the range of local annual mean high and low tides, being of most effective use by enclosing maximum amount of water at mid-tide. Structures N4 and N5 are constructed on elevated topography above AHD, making the traps effective during the higher magnitudes of present mid-tidal conditions. As structures drop below working range with receding tides, the enclosed areas are left effectively dry, and N1, N2, N3, N7 and K4, K5, K6 located on lower elevations near or below AHD, come into effect (Fig. 8, Fig. S2). N7, with the greatest height of 0.98 m, is the only structure with sufficient height to extend its working range across mid and low magnitude tides. When assessing simultaneous inundation of fishtraps, it is evident that the greatest number of fishtraps are effective near PMSL. Trap use at mid-tide is further supported by ethnographic accounts of Kaiadilt paying daily visits to a fishtrap near camp at mid-tide (Tindale, 1962b). The documented fishtrap sites suggest two groups of stone-walled features operating in two intertidal zones, differentiated by approximately 0.5 m in elevation (Fig. S3), which may indicate a construction strategy that optimises the potential of enclosing marine resources during mid-tide across various tidal cycles.

With the variety of tidal patterns in the southern Gulf of Carpentaria, the island group is exposed to fluctuating tidal magnitude and frequency throughout the year (Forbes and Church, 1983). To assess seasonal functionality of the stone-walled structures, the observed mean high and low tide of two consecutive months representative of the wet (December–January) and dry (June–July) seasons were calculated. While tidal range was not predicted to significantly alter across seasons (0.02 m greater in the wet season), the shore inundation is less in the drier months. However, with the positioning and height of the documented fishtraps, working range is not impacted by seasonal tidal oscillations. Under average tidal conditions, the structures are most effective during high-to-mid-tide in the dry season, while mid-to-low tide provides optimal conditions during the wet (Fig. 9).

4.4. Past sea-level conditions

Geomorphological studies demonstrate peak sea-levels of +1.5 m-2 m between 7700 and 4000 cal BP before receding to current levels (Sloss et al., 2018). Past sea-levels were modelled at magnitudes up to +2 m greater than PMSL. An average tidal range relative to current regimes was assumed for modelling purposes and demonstrated that all structures would be submerged at mean sea-level. Only trap N4, anchored to the current high water mark, could have been of semi-effective use at the lowest tide (Fig. S4). With sea-levels receding to +1 m greater than PMSL, all fishtraps are situated within the tidal range, but only effective during low tides (Fig. S5). When comparing fishtrap function at current and enhanced sea-levels, the structural ability of controlling water movement is optimal, with the largest number of traps within working range at current, or close to current, sea-levels (Fig. 10). The individual and simultaneous function throughout PMSL tidal cycles indicates a late Holocene antiquity for the 13 fishtraps documented in this study area; aligning with the human occupation signal across the archipelago (Memmott et al., 2016).

5. Discussion

5.1. Fishtrap operation and construction

The GIS-generated sea-level scenarios demonstrate that the stone-walled structures of Ngathald and Kabar Bays would not have had effective working ranges prior to c.3500 cal BP, which correlates with the earliest occupation dates of Sweers and Bentinck Islands dating to c.3500 cal BP (Memmott et al., 2016). With a continuous signal of occupation from c.2000 cal BP in the archipelago, and ethnographic

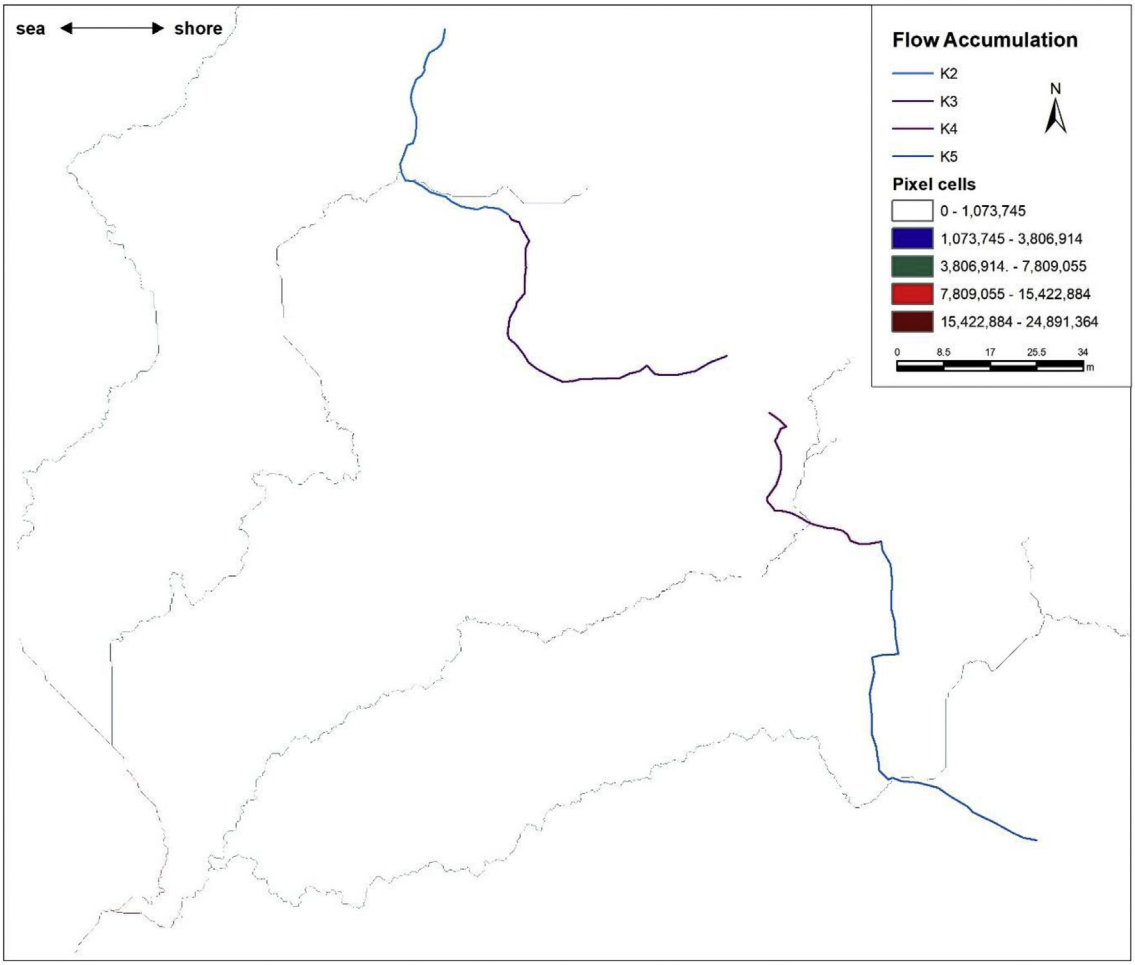

Fig. 7. Example of the flow accumulation output, demonstrating flow direction towards the sea based on topography underlying four stone-walled fishtraps. Flow accumulation is expressed in accumulated flow to each pixel cell, where a greater number of cells represents greater accumulation. Although the low gradient topography demonstrates a faint signal, with relatively low cell counts of accumulated flow, it is evident that the structures K2, K4 and K5 have a single course of water flow, situated beneath or near the most seaward point of the structure.

records outlining the need for ongoing fishtrap maintenance for optimal function (e.g. Tindale, 1960), it can be concluded that the fishtraps were constructed within the last two millennia. With the current fishtrap placement and a consistent trap height below 1 m, the traps of Ngathald and Kabar Bays would have functioned with tides 0.5 m ± PMSL. With the relatively narrow fishtrap working range, sea-level shifts of ± 0.5 m would have a significant impact on trap function. As further refined high-resolution regional and local sea-level curves become available it will be possible to further refine construction chronologies. It is acknowledged that trap height may have decreased over time, however as such erosion cannot be demonstrated without long-term monitoring of fishtrap morphology, analysis is based on the properties of current structures.

Based on the findings of fishtrap construction and interaction with past and current tidal regimes, we recommend high-resolution documentation of fishtrap metrics (length, height, width), particularly elevation in relation to a national height datum. While the method and majority of the analytical procedure can be applied to other archaeological site types, photogrammetric UAV recording proved particularly useful for documenting features in the intertidal zone. Previous fishtrap documentation has varied in detail, and cross-site comparison is limited due to ambiguous descriptions. GIS assessment of fishtrap physical features enabled quantitative analysis of geometric properties and formed a basis for robust comparative studies. By describing the structures through geometric variables, the risk of misidentification is minimised and the potential for site comparison and modelling maximized. Simple yet inclusive terms, such as fishtraps, representing structures (natural or constructed) enclosing bodies of water, described by metric properties is recommended to move towards a standardised objective industry practice. To further knowledge of the site type, geomorphological studies of environmental impacts on local ecosystems within the structures will assist in understanding local resource management, and potential erosion and sedimentation impacts on the wider intertidal zone. Such recent and historical information, of structural function and environmental impact, can contribute to development of site-specific cultural heritage management plans for stone-walled features in low energy intertidal environments. Evidence of local marine resource technologies, and their impacts, will further allow indicators of concepts such as domestication, cultural niche constructions, and potential aquaculture paradigms, to be evaluated and explored further.

5.2. Data acquisition and processing

Documenting large-scale remote archaeological structures through photogrammetric UAV survey proved to be a time effective recording procedure. The intertidal zone, with particular environmental constraints and wildlife hazards, make pedestrian recording difficult. Through UAV documentation, the entire area was captured in great detail without disturbing the site or archaeological features. The birds-eye perspective proved vital to accurately assess the contextual landscape in which fishtraps are situated, including relationships between

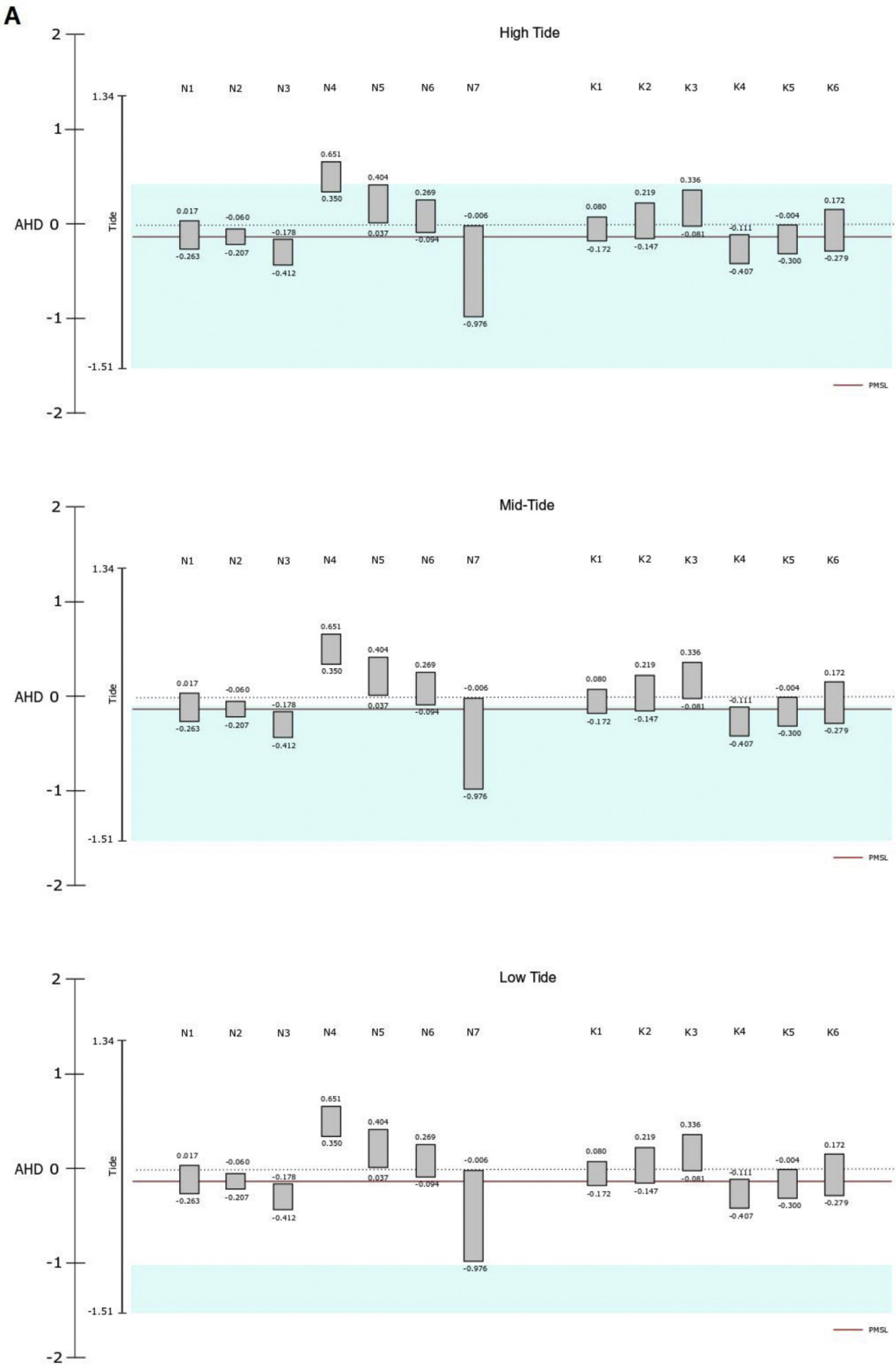

Fig. 8. Effects of an outgoing tide on stone-walled intertidal fishtraps, illustrated by (A) cross-sections and (B) vectorized high tide (HT), mid-tide (MT), and low tide (LT) mean tides of 2015, overlayed on digitized Ngathald Bay fishtraps and the UAV-captured orthographic image. During high tide, all structures are inundated by water and have exceeded their working range. At mid-tide, structure N4 is the first to come in effect, followed by other structures (N5, K3, N6 etc). While higher elevated structures drop below their working range with the receding tide, others come into effect, leaving N7 to be the last trap out of working range during low tide.

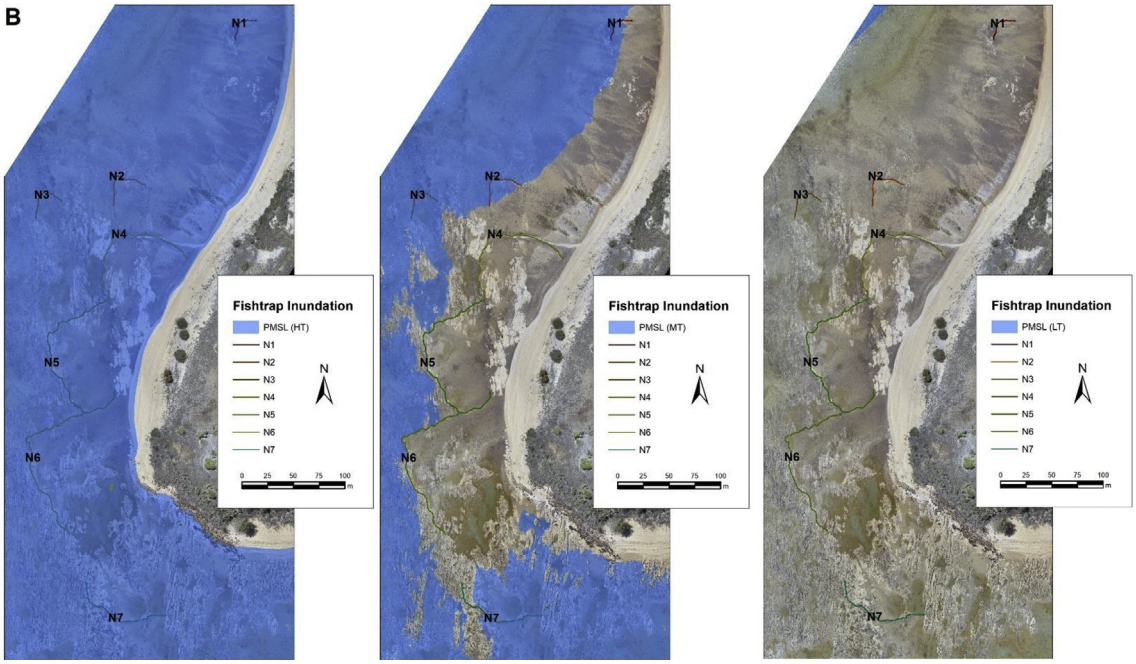

Fig. 8. (*continued*)

features, which cannot be easily or accurately identified from a horizontal perspective. The method provided objective data collection, enabling post-collection analysis and interpretation not exclusively based on the initial judgement of the recorder. The highly accurate dataset further provides certainty in the results presented, and potential for future expansion of the analytical procedure presented in this research. Recording elevation in relation to AHD further aligns with Australian geographic survey standards (Intergovernmental Committee on Surveying and Mapping, 2014) and enables nation-wide site comparison if adopted in future site documentation. While the recording procedure required licensed pilots due to UAV weight class regulations under the CASA legislation (CASA, 2018), and data processing required some professional training, the method is relatively user-friendly, affordable, and accessible. Despite the compelling advantages of recording fishtraps utilising UAV and close-range photogrammetry, prevailing intertidal conditions and the high-resolution data acquisition presented some challenges.

While the approach provides a high accuracy output at a very high-resolution of a large-scale site – required for water pooling analysis of low-energy intertidal zones – weather, time, and hardware availability govern the application. Studies of intertidal site types will be subjected to weather and tidal restrictions, and despite the custom-made octocopter's technical capability of flying in winds up to 47 km/h, such conditions compromise flight time and pose a significant challenge for accessing intertidal sites, especially by boat. Tidal movement and daylight further restricted the time available for recording. The stone-walled structures were recorded at low tide, which set a limited timeframe, further constrained by low tides occurring in late hours of the

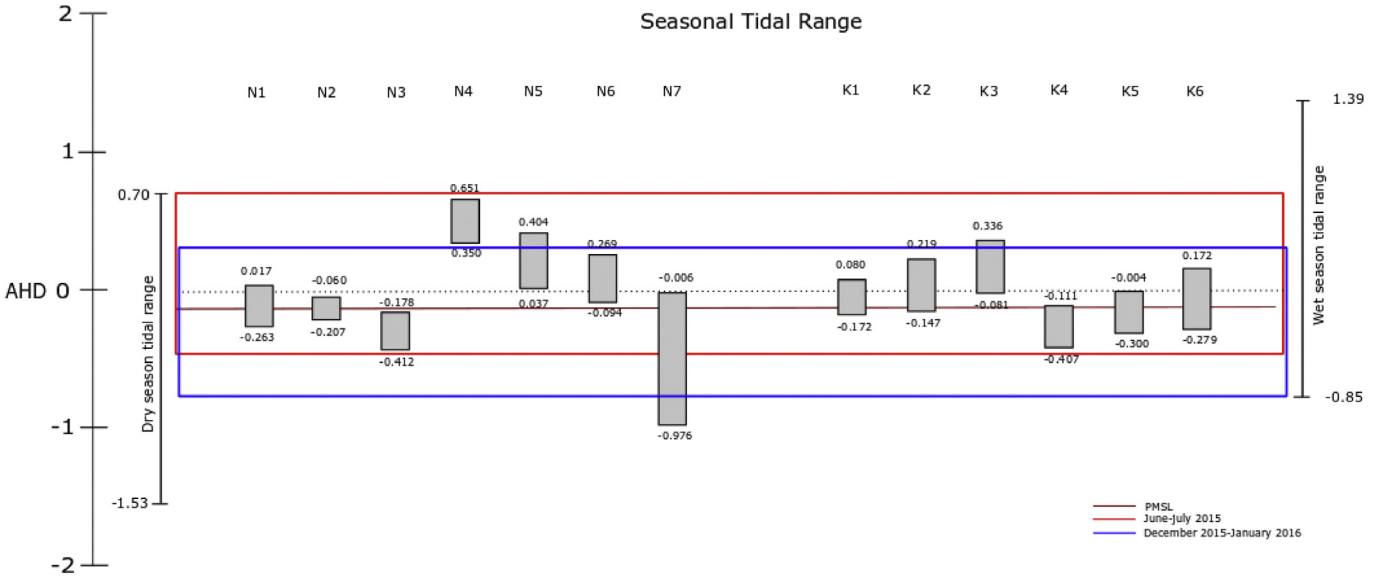

Fig. 9. Fishtrap function during mean tidal conditions in June/July 2015 and December 2015/January 2016, representative of the dry and wet seasons respectively, with the most effective timeframe of enclosing water indicated in red and blue. In the dry season, structures are of most effective use during high-to-mid-tides, while mid-to-low tidal conditions are more effective in wetter months. (For interpretation of the references to colour in this figure legend, the reader is referred to the Web version of this article.)

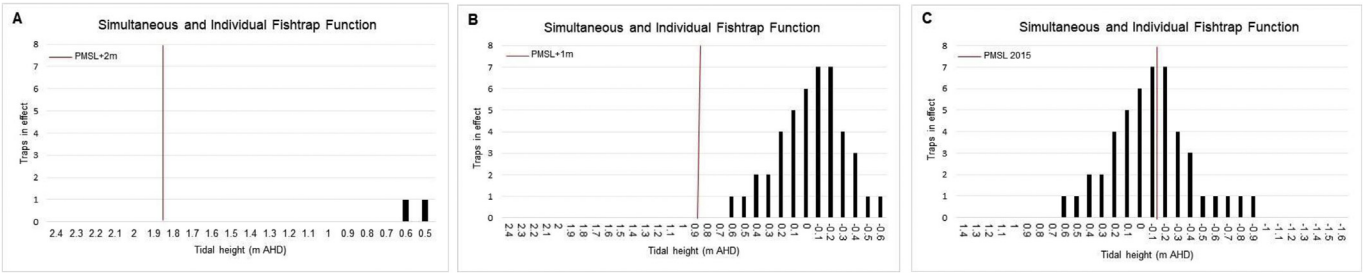

Fig. 10. Number of traps in effect at 0.1 m tidal height increments. (A) When modelling PMSLs at a 2 m greater magnitude, during a relative mean tidal range similar to current tidal conditions, a single fishtrap comes into effect at the end of the diurnal tidal cycle at elevations below 0.6 m AHD. (B) At PMSLs enhanced by 1 m, a maximum of 7 fishtraps are predicted to simultaneously hold water during low tide, and (C) assessment of the simultaneous function of stone-walled structures demonstrate individual fishtraps to enclose bodies of water most effectively at current, or close to, present sea-levels.

day which reduced available daylight. Data acquisition during the lowest possible tide was necessary, as water causes the DEM to calculate elevation values of the water surface, or refracted through the surface, rather than directly off the underlying topography. Specular reflection and wave action can further result in *null* values, displayed as 'holes' in the raster surface. Very shallow areas of water were present within a few traps during recording of the Sweers Island sites. However, with such minor occlusion areas, the surface extrapolation during the DEM generation provide accurate surface values across site. While the demonstrated time restrictions are a result of the intertidal site type, rather than the recording method, distributing GCPs was the most time-consuming aspect of the UAV methodology; a routine now eliminated by mounting a compact RTK GNSS system to the UAV.

High-resolution low-level aerial imagery further presented some challenges in file size and processing time. Data processing was performed on a workstation, equipped with an 8 Core Intel CPU, dual nVidia 4 GB GTX980 graphic cards and 128 GB RAM, generating a 63.5 GB dataset of the recorded Sweers Island sites, computed over approximately 160 h. The analytical procedure was performed on a desktop of the same capabilities, where individual GIS operations required no more than 2 min to generate, with the exception of flow accumulation which computed over 1.5 h. However, analysing such a dataset with hardware of less graphic capacity will require a substantially longer timeframe.

Subjectivity in the manual digitisation of fishtraps was the final challenge of the post-processing procedure. To exclude subjectivity of the digitiser, object-based image analysis (OBIA) was considered, a well-established technique in remote sensing and geomorphological research (e.g. Blaschke, 2010; Conrad et al., 2015). While the technique initially showed promising results for identifying fishtraps in open source software System for Automated Geoscientific Analysis (v.2.2.7), the large file size hindered the system to perform image segmentation required to assess recognisable features across the assemblage. Instead, subjectivity was minimised by performing analysis in ArcMap by a single digitiser, applying *heads-up* digitisation (regularly using the zoom feature and multiple generated layers) to consider context as well as fine-scaled components affecting the capability of stone-walled structures to enclose water. Cross-referencing with the orthographic image proved crucial in digitisation of fishtraps, as the high-resolution image displayed discrepancies in low-gradient features that computed operations were unable to distinguish. For instance, walls near shore appear to be inundated by sediment, creating a flat appearance of the surface that could mislead length measurements; a natural process that may have altered through time, but unable to be detected by outputs such as contour and slope.

The analytical procedure and model validity presented in this study can further be improved by utilising a local port datum (when available), accurately reflecting the fluctuating tidal regime, particularly to provide information on out of the ordinary tidal events. Utilising the DEM output to its full potential can enable volume calculations (m^3) of fishtrap holding capacity across sites. Analysis of enclosed submerged surface area during various tidal heights will shine further light on fishtrap placement and test the importance of shape characteristics. Understanding fishtrap holding capacity will contribute to discussions of resource management. Finally, to reach standardised, quantitative analytical procedures of archaeological site types, OBIA and pattern recognition software should be further trialled.

5.3. Fishtrap terminology

The GIS analysis supported previous findings of challenges in inconsistent fishtrap terminology, particularly where focus is placed on shape features (Rowland and Ulm, 2011). The elevation range of the Ngathald and Kabar Bay fishtrap placement, in conjunction with the flow accumulation output, provide strong indication that structures are shaped to control the movement of marine resources with receding tides (Fig. S6, Fig. S7). Flow direction may lead structures to have a V or U appearance, however, results indicate function as a driver of construction, rather than stylistic choice. While this may not be a surprising find, it demonstrates the strengths of adopting metric-focused terminology, rather than morphological descriptions, and provides the basis for a less subjective interpretation of fishtrap construction and function. Accurate geometric classifications of fishtraps proved crucial in producing a replicable analytical procedure and perform a standardised analysis across structures.

6. Conclusion

The highly accurate dataset obtained through high-resolution UAV photogrammetric mapping of Ngathald and Kabar Bays, Sweers Island, identified 13 Kaiadilt fishtraps, where local topography was determined to be the dominant consideration in fishtrap placement and construction. The intertidal locations effectively enable operation of the fishtraps all year around, and elevations of the stone-walled constructions place them at optimal use during PMSL. During times of increased sea-levels, the structures have capacity to be of effective use during low tide in magnitudes up to +1 m above PMSL, and combined with archaeological records, indicate a construction date in the last 2000 years. The UAV documentation technique and GIS analysis presented in this study provides the basis for further refinement of the chronology of construction when higher-resolution regional sea-level histories are available for the late Holocene. Considering fishtrap working range during past sea-levels is the most recent, viable option to date stone-walled fishtraps located in the present intertidal zone. The impact of future sea-level rise on fishtraps can also be modelled for mitigation and cultural heritage management applications. Aligning recording methods and terminology to a standardised quantitative technique will further benefit management plans for preservation of the site type and contribute to a broader cross-disciplinary understanding of stone-walled intertidal fishtrap.

Acknowledgements

We acknowledge Kaiadilt traditional owners of the South Wellesley Islands as partners in this research. The Kaiadilt Aboriginal Corporation collaborated in establishing the research framework for this project and have approved publication of this research. We extend a special thanks to Michael Boland for his UAV expertise, Tex and Lyn Battle, Brett Jeffries, Sarah Jae Martin, and Karen Gadsby for logistical assistance. We thank Michael Rowland and Ian McNiven for comments on an earlier version of this manuscript. This research was conducted by the Australian Research Council Centre of Excellence for Australian Biodiversity and Heritage (CE170100015). The project was supported under the Australian Research Council's Discovery Projects funding scheme (project number DP120103179), Scarp Archaeology's Richard Brookdale Scholarship, and Australian Association of Consulting Archaeologists Inc. Student Support Fund 2015. SU is the recipient of an Australian Research Council Future Fellowship (project number FT120100656). Work on this paper was undertaken while SU was visiting as an Honorary Fellow in the School of Social Sciences, The University of Western Australia.

Appendix A. Supplementary data

Supplementary data related to this article can be found at https://doi.org/10.1016/j.jas.2018.05.012.

References

Baltsavias, E.P., 1999. A comparison between photogrammetry and laser scanning. ISPRS J. Photogrammetry Remote Sens. 54 (2–3), 83–94. https://doi.org/10.1016/S0924-2716(99)00014-3.

Bannerman, N., Jones, C., 1999. Fish-trap types: a component of the maritime cultural landscape. Int. J. Naut. Archaeol. 28 (1), 70–84. https://doi.org/10.1111/j.1095-9270.1999.tb00823.x.

Blaschke, T., 2010. Object based image analysis for remote sensing. ISPRS J. Photogrammetry Remote Sens. 65 (1), 2–16. https://doi.org/10.1016/j.isprsjprs.2009.06.004.

Builth, H., 2014. Ancient Aboriginal Aquaculture Rediscovered: the Archaeology of an Australian Cultural Landscape. Saarbruken: LAP LAMBERT Academic Publishing.

Bureau of Meteorology, 2018. Monthly sea-levels for Karumba - 1985 to 2016. Retrieved 19 March 2018 from. http://www.bom.gov.au/ntc/IDO70000/IDO70000_63580_SLD.shtml.

Caldwell, M., Lepofsky, D., Combes, G., Washington, M., Welch, J.R., Harper, J.R., 2012. A bird's eye view of Northern Coast Salish intertidal resource management features, southern British Columbia, Canada. J. I. Coast Archaeol. 7 (2), 219–233. https://doi.org/10.1080/15564894.2011.586089.

Campbell, J.B., 1982. Automatic seafood retrieval systems: the evidence from Hinchinbrook Island and its implications. In: Bowdler, S. (Ed.), Coastal Archaeology in Eastern Australia. Department of Prehistory, Research School of Pacific Studies, Australian National University, Canberra, pp. 96–107.

Civil Aviation Safety Authority (CASA), 2018. Flying Drones/Remotely Piloted Aircraft in Australia. Retrieved 19 March 2018 from. https://www.casa.gov.au/aircraft/landing-page/flying-drones-australia.

Codding, B.F., Bird, D.W., 2015. Behavioral ecology and the future of archaeological science. J. Archaeol. Sci. 56, 9–20. https://doi.org/10.1016/j.jas.2015.02.027.

Connah, G., Jones, A., 1983. Aerial archaeology in Australia. Aerial Archaeol. 9, 1–23.

Conrad, O., Bechtel, B., Bock, M., Dietrich, H., Fischer, E., Gerlitz, L., Wehberg, J., Wichmann, V., Böhner, J., 2015. System for automated geoscientific analyses (SAGA) v. 2.1. 4. Geosci. Model Dev. (GMD) 8 (7) 1991-2007. https://doi.org/10.5194/gmd-8-1991-2015.

Coutts, P.J.F., Franks, R.K., Hughes, P., 1978. Aboriginal Engineers of the Western District, Victoria. Records of the Victorian Archaeological Survey 7. Ministry for Conservation, Melbourne.

Department of Transport and Main Roads, 2013. Inscription Point Sweers Island 2013. Commonwealth of Australia. Retrieved 4 May 2016 from. https://www.msq.qld.gov.au/-/media/MSQInternet/MSQFiles/Home/Tides/sweersislandtidepredictions.pdf?la=en.

Department of Transport and Main Roads, 2017. Queensland Tide Tables Standard Port Tide Times 2018. Maritime Safety, Queensland, Brisbane.

De Reu, J., Plets, G., Verhoeven, G., De Smedt, P., Bats, M., Cherretté, B., De Maeyer, W., Deconynck, J., Herremans, D., Laloo, P., 2013. Towards a three-dimensional cost-effective registration of the archaeological heritage. J. Archaeol. Sci. 40 (2), 1108–1121. https://doi.org/10.1016/j.jas.2012.08.040.

Doneus, M., Doneus, N., Briese, C., Pregesbauer, M., Mandlburger, G., Verhoeven, G., 2013. Airborne laser bathymetry - detecting and recording submerged archaeological sites from the air. J. Archaeol. Sci. 40, 2136–2151. https://doi.org/10.1016/j.jas.2012.12.021.

Dortch, C., 1997. New perceptions of the chronology and development of Aboriginal fishing in south-western Australia. World Archaeol. 29 (1), 15–35. https://doi.org/10.1080/00438243.1997.9980361.

Dortch, J., Dortch, C., Reynolds, R., 2006. Test excavation at the Oyster Harbour stone fish traps, King George Sound, Western Australia: an investigation aimed at determining the construction method and maximum age of the structures. Aust. Archaeol. 62, 38–43. https://doi.org/10.1080/03122417.2006.11681829.

Elder, J.T., Gilmour, D.M., Butler, V.L., Campbell, S.K., Steingraber, A., 2014. On the role of coastal landscape evolution in detecting fish weirs: a Pacific Northwest coast example from Washington State. J. I. Coast Archaeol. 9 (1), 45–71. https://doi.org/10.1080/15564894.2014.881933.

Evans, N.D., 1995. A Grammar of Kayardild. Mouton de Gruyter, Berlin.

Forbes, A., Church, J., 1983. Circulation in the Gulf of Carpentaria. II. Residual currents and mean sea level. Aust. J. Mar. Freshw. Res. 34 (1), 11–22. https://doi.org/10.1071/MF9830011.

Geoscience Australia, 2018. Australian Height Datum. Retrieved 17 March 2018 from. http://www.ga.gov.au/scientific-topics/positioning-navigation/geodesy/ahdgm/ahd.

Greene, N.A., McGee, D.C., Heitzmann, R.J., 2015. The Comox Harbour fish trap complex: a large-scale, technologically sophisticated intertidal fishery from British Columbia. Can. J. Archaeol. 39 (2), 161–212.

Intergovernmental Committee on Surveying and Mapping, 2014. Standard for the Australian Survey Control Network: Special Publication 1 (v.2.1). Commonwealth of Australia, Canberra.

Jeffery, B., 2013. Reviving community spirit: furthering the sustainable, historical and economic role of fish weirs and traps. J. Marit. Archaeol. 8 (1), 29–57. https://doi.org/10.1007/s11457-013-9106-4.

Koivisto, S., Latvakoski, N., Perttola, W., 2018. Out of the peat: preliminary geophysical prospection and evaluation of the mid-Holocene stationary wooden fishing structures in Haapajärvi, Finland. J. Field Archaeol. 43 (3), 166–180. https://doi.org/10.1080/00934690.2018.1437315.

Kuhn, M., Tuladhar, D., Corner, R., 2011. Visualising the spatial extent of predicted coastal zone inundation due to sea level rise in south-west Western Australia. Ocean Coast Manag. 54 (11), 796–806. https://doi.org/10.1016/j.ocecoaman.2011.08.005.

Langouët, L., Daire, M.Y., 2009. Ancient maritime fish-traps of Brittany (France): a re-appraisal of the relationship between human and coastal environment during the Holocene. J. Marit. Archaeol. 4 (2), 131–148. https://doi.org/10.1007/s11457-009-9053-2.

Lepofsky, D., Caldwell, M., 2013. Indigenous marine resource management on the northwest coast of north America. Ecol. Process. 2 (1), 1–12. https://doi.org/10.1186/2192-1709-2-12.

Lichter, M., Felsenstein, D., 2012. Assessing the costs of sea-level rise and extreme flooding at the local level: a GIS-based approach. Ocean Coast Manag. 59, 47–62. https://doi.org/10.1016/j.ocecoaman.2011.12.020.

Lourandos, H., 1980. Change or stability?: Hydraulics, hunter-gatherers and population in temperate Australia. World Archaeol. 11 (3), 245–264. https://doi.org/10.1080/00438243.1980.9979765.

Lourandos, H., 1983. Intensification: a late Pleistocene-Holocene archaeological sequence from southwestern Victoria. Archaeol. Ocean. 18 (2), 81–94.

McCoy, M.D., Asner, G.P., Graves, M.W., 2011. Airborne lidar survey of irrigated agricultural landscapes: an application of the slope contrast method. J. Archaeol. Sci. 38 (9), 2141–2154. https://doi.org/10.1016/j.jas.2011.02.033.

McNiven, I.J., Crouch, J., Richards, T., Gunditj Mirring Traditional Owners Aboriginal Corporation, Dolby, N., Jacobsen, G., 2012. Dating Aboriginal stone-walled fish traps at Lake Condah, southeast Australia. J. Archaeol. Sci. 39 (2), 268–286. https://doi.org/10.1016/j.jas.2011.09.007.

McNiven, I.J., Crouch, J., Richards, T., Sniderman, K., Dolby, N., Mirring, Gunditj, 2015. Phased redevelopment of an ancient Gunditjmara fish trap over the past 800 years: Muldoons trap complex, Lake Condah, southwestern Victoria. Aust. Archaeol. 81, 44–58. https://doi.org/10.1080/03122417.2015.11682064.

Memmott, P., 1982. The South Wellesley Islands and the Kaiadilt: a History and an Analysis of the Significance of the Land and its People. Unpublished Manuscript, Aboriginal Data Archive. Department of Architecture, The University of Queensland, Brisbane.

Memmott, P., Robins, R., Stock, E., 2008. What exactly is a fish trap? Methodological issues for the study of Aboriginal intertidal rock-wall fish traps, Wellesley Islands region, Gulf of Carpentaria, Australia. In: Conolly, J., Campbell, M. (Eds.), Comparative Island Archaeologies. Oxford: Archaeopress, pp. 47–67 BAR International Series S1829.

Memmott, P., Round, E., Rosendahl, D., Ulm, S., 2016. Fission, fusion and syncretism: linguistic and environmental changes amongst the Tangkic people of the southern Gulf of Carpentaria, northern Australia. In: Verstraete, J.-C., Hafner, D. (Eds.), Land and Language in Cape York Peninsula and the Gulf Country. John Benjamins Publishing Company, Amsterdam, pp. 105–136. Culture and Language Use 18. https://doi.org/10.1075/clu.18.06mem.

Moss, M.L., Erlandson, J., Bernick, K.N., 1998. A Comparative Chronology of Northwest Coast Fishing Features. University of British Columbia Press, Vancouver.

Olson, B.R., Placchetti, R.A., Quartermaine, J., Killebrew, A.E., 2013. The Tel Akko Total Archaeology Project (Akko, Israel): assessing the suitability of multi-scale 3D field recording in archaeology. J. Field Archaeol. 38 (3), 244–262. https://doi.org/10.1179/0093469013Z.00000000056.

O'Sullivan, A., 2004. Place, memory and identity among estuarine fishing communities: interpreting the archaeology of early medieval fish weirs. World Archaeol. 35 (3), 449–468. https://doi.org/10.1080/0043824042000185810.

Peck, H., 2016. The Application of Ecological Models and Trophic Analyses to Archaeological Marine Fauna Assemblages: towards Improved Understandings of

Prehistoric Marine Fisheries and Ecosystems in Tropical Australia. Unpublished PhD thesis. College of Arts, Society and Education, James Cook University, Cairns.
Richards, T., 2013. Transegalitarian Hunter-Gatherers of Southwest Victoria, Australia. Unpublished PhD thesis. School of Geography and Environmental Science, Monash University, Melbourne.
Roberts, A., Mollenmans, A., Agius, Q., Graham, F., Newchurch, J., Rigney, L.-I., Sansbury, F., Sansbury, L., Turner, P., Wanganeen, G., 2016. "They planned their Calendar… They set up ready for what they wanted to feed the tribe": a first-stage analysis of Narungga fish traps on Yorke Peninsula, South Australia. J. I. Coast Archaeol. 11 (1), 1–25. https://doi.org/10.1080/15564894.2015.1096869.
Robins, R.P., 1983. Report on a Preliminary Archaeological Reconnaissance of Sweers Island, 24–25 August 1982. Unpublished report prepared for Moyenda Association, Mornington Island. .
Ross, P.J., 2009. Ngarrindjeri Fish Traps of the Lower Murray Lakes and Northern Coorong Estuary, South Australia. Unpublished Masters (Maritime Archaeology) thesis. Department of Archaeology, Flinders University of South Australia, Adelaide.
Rowland, M.J., Ulm, S., 2011. Indigenous fish traps and weirs of Queensland. Queensl. Archaeol. Res. 14, 1–58. http://doi.org/10.25120/qar.14.2011.
Rowland, M.J., Ulm, S., Roe, M., 2014. Approaches to monitoring and managing Indigenous Australian coastal cultural heritage places. Queensl. Archaeol. Res. 17, 37–48. http://doi.org/10.25120/qar.17.2014.231.
Saenger, P., Hopkins, M., 1975. Observations on the Mangroves of the South-eastern Gulf of Carpentaria. Report prepared for Environment Science and Services North Brisbane.
Sapirstein, P., 2016. Accurate measurement with photogrammetry at large sites. J. Archaeol. Sci. 66, 137–145. https://doi.org/10.1016/j.jas.2016.01.002.
Sloss, C.R., Nothdurft, L., Hua, Q., O'Connor, S.G., Moss, P.T., Rosendahl, D., Petherick, L.M., Nanson, R.A., Mackenzie, L.L., Sternes, A., Jacobsen, G.E., Ulm, S., 2018. Holocene Sea-level Change and Coastal Landscape Evolution in the Southern Gulf of Carpentaria, Australia. The Holocene. in press. https://doi.org/10.1177/0959683618777070.
Smith, B.D., 2014. Documenting human niche construction in the archaeological record. In: Marston, J.M., D'Alpoim Guedes, J., Warinner, C. (Eds.), Method and Theory in Paleoethnobotany. University Press of Colorado, Colorado, pp. 355–370.
Smith, M., 1987. Dots on the map: sites and seasonality, the Bardi example. Aust. Archaeol. 25, 40–52.
Stockton, J., 1975. An Aboriginal fishtrap from southern Queensland. Mankind 10 (1), 44–47. https://doi.org/10.1111/j.1835-9310.1975.tb00912.x.
Tindale, N.B., 1960. Journal of Visit to Bentinck and Mornington Island. South Australian Museum, Queensland. Adelaide Pagination as per typescript copy held in S.A. Museum.
Tindale, N.B., 1962a. Geographic knowledge of the Kaiadilt people of Bentinck Island, Queensland. Record S. Aust. Mus. 14, 259–296.
Tindale, N.B., 1962b. Some population changes among the Kaiadilt people of Bentinck Island, Queensland. Record S. Aust. Mus. 14, 297–318.
Ulm, S., Evans, N., Rosendahl, D., Memmott, P., Petchey, F., 2010. Radiocarbon and linguistic dates for occupation of the South Wellesley Islands, northern Australia. Archaeol. Ocean. 45 (1), 39–43. https://doi.org/10.1002/j.1834-4453.2010.tb00076.x.
United States Geological Survey, 2017. USGS Global Positioning Application and Practice. Retrieved 17 April 2018 from. https://water.usgs.gov/osw/gps/.
Van Waarden, N., Wilson, B., 1994. Developing a hydrological model of the Lake Condah fish traps in western Victoria using GIS. In: Johnson, I. (Ed.), Methods in the Mountains. Archaeological Computing Laboratory, Department of Prehistoric and Historical Archaeology, The University of Sydney, Sydney, pp. 81–90 Sydney University Archaeological Methods Series 2.
Verhoeven, G., 2011. Taking computer vision aloft-Archaeological three-dimensional reconstructions from aerial photographs with PhotoScan. Archaeol. Prospect. 18 (1), 67–73. https://doi.org/10.1002/arp.399.
Zeder, M.A., 2015. Core questions in domestication research. Proc. Natl. Acad. Sci. Unit. States Am. 112 (11), 3191–3198. https://doi.org/10.1073/pnas.1501711112.